Ignition delay study of aluminium oxide liquid nano-fuel in a shock tube

D. K. Tripathi[1], G. Garg[2], U. Agrawal[2], V. Menezes[1,*], U. V. Bhandarkar[2] and B. P. Puranik[2]

[1]Department of Aerospace Engineering, and
[2]Department of Mechanical Engineering, Indian Institute of Technology Bombay, Powai, Mumbai 400 076, India

The ignition delay of aluminium oxide (Al$_2$O$_3$) liquid nano-fuel was compared with that of base-fuel to study the feasibility of its use for high-speed aerospace applications. The base-fuel was aviation turbine fuel that was mixed with Al$_2$O$_3$ nanoparticles to produce a nano-fuel which could be used for regenerative cooling of the combustor walls before injection. The experiments were carried out in a shock tube. The fuel was introduced into the shock tube in the form of a wall droplet. The ignition delay time of the nano-fuel was observed to increase slightly, by about 11% (maximum) in comparison with the baseline, at an equivalence ratio of unity.

Keywords: Aluminium oxide, ignition delay, liquid nano-fuel, shock tube.

IGNITION delay sets the residence time of a fuel in the combustion chamber of a high-speed engine, and is a useful parameter in determining the capability of ignition and flame sustainability in a flow where a packet of air–fuel mixture resides for a few milliseconds[1]. Estimation of ignition delay of a fuel produced for high-speed operations is essential to avoid fluctuations in energy release and specific impulse of the engine.

Aviation turbine fuel (ATF) is a preferred hydrocarbon fuel owing to its high energy density and stable thermodynamic properties. We produced a fuel by mixing ATF with alumina (Al$_2$O$_3$) nanoparticles for the dual purpose of regenerative cooling of combustor walls and preheating the fuel before injection. Heat transfer studies have indicated an increase between 20% and 30% in the heat transfer coefficient with 0.3% volume fraction loading of Al$_2$O$_3$ nanoparticles[2]. The nano-fuel has a probable application in high-speed engines, such as pulse detonation engines. The objective of the present study was to confirm that the ignition delay of the admixture was within the acceptable limits.

The experiments were carried out in a shock tube of variable inner diameter (i.d.). The inner diameter and length of the driver and driven sections of the tube were 51 mm, 37 mm and 2.5 m, 3 m respectively. Figure 1 shows a schematic of the experimental set-up. The test gas was air, which was maintained at an appropriate pressure for the test in the driven section of the tube. The driver and driven sections were separated by an aluminium diaphragm (1.2 mm thickness) that was exploded by pressurization of the driver section by purified nitrogen gas. The explosion launched an incident shock wave into the driven section that propagated through the test gas and reflected from the driven-end, enhancing the shocking effect. The propagation of the planar shock waves finally left behind a reservoir of high temperature and pressure in the driven section, which could simulate a combustor for the study of ignition characteristics of fuels. The liquid fuel to be tested was preloaded into the end of the driven section as a wall droplet, which was atomized on collision with the propagating shock waves. The propagating shock waves accomplished the function of a fuel injector in the present case[3]. The Mach number of the incident shock wave was modulated to obtain the desired test conditions.

The shock tube consisted of pressure transducers/gauges and a photodiode to measure the pressure and photonic output during the ignition tests. The pressure transducers were flush-mounted in the tube wall at the end of the driven section, whereas the photodiode was mounted on the external surface of the driven-end flange that had an acrylic optical window of 35 mm diameter to transmit light during ignition. The pressure transducers (PCB-Piezotronics, USA) had sensitivities and peak loading limits of 1 and 5 mV/psi, and 5000 and 1000 psi (models 102B and 102B04) respectively. The photodiode (model PDA36A-EC, THORLABS, USA) had an operating wavelength bandwidth of 350–1100 nm and an adjustable gain of 0–70 dB. The signals from the sensors were acquired on a PC-based data acquisition system with NI PCI-6115 S data cards (National Instruments, USA), at a sampling rate of 1 MS/s. The images of fuel ignition were obtained using Phantom V 710 high-speed video camera, with sampling rate and spatial resolution of 64 kfps and 320 × 240 pixels respectively.

Figure 2 presents the output of the tube-end pressure transducer (S_2) and photodiode for dry runs (without fuel). The first jump in the pressure marks the arrival of the incident shock wave at S_2, and the next jump indicates the arrival of the reflected shock wave from the tube end. The output of the photodiode did not show any rise during the dry run. The Mach number of the incident shock wave (M_S) can be calculated using eq. (1), with the pressure jump across the incident shock wave (P_1 to P_2) and γ (ratio of the specific heat capacities of test gas, i.e. air)[4]

$$M_S = \sqrt{\frac{\gamma+1}{2\gamma}\left(\frac{P_2}{P_1}-1\right)+1}. \tag{1}$$

The temperature across the moving shock wave can be calculated using eq. (2), where T_a and T_b are the temperature ahead and behind the shock wave, and P_a and P_b are

Table 1. Test conditions in the shock tube for dry runs (without fuel)

Driver gas	M_s	P_1 (bar)	P_2 (bar)	P_5 (bar)	T_5 (K)
Nitrogen	2.065 ± 1.2%	1	4.41 ± 2.5%	17.5 ± 4%	805.4 ± 2.8%
Nitrogen	2.074 ± 1.9%	0.8	3.89 ± 3.9%	16.6 ± 5.1%	872.6 ± 2.4%

Test gas, Air; M_s, Incident shock Mach number; P, Pressure; T, Temperature. Suffix – 1, Initial condition; 2, Across incident shock wave and 5, Across reflected shock wave. Scatter indicates standard deviation.
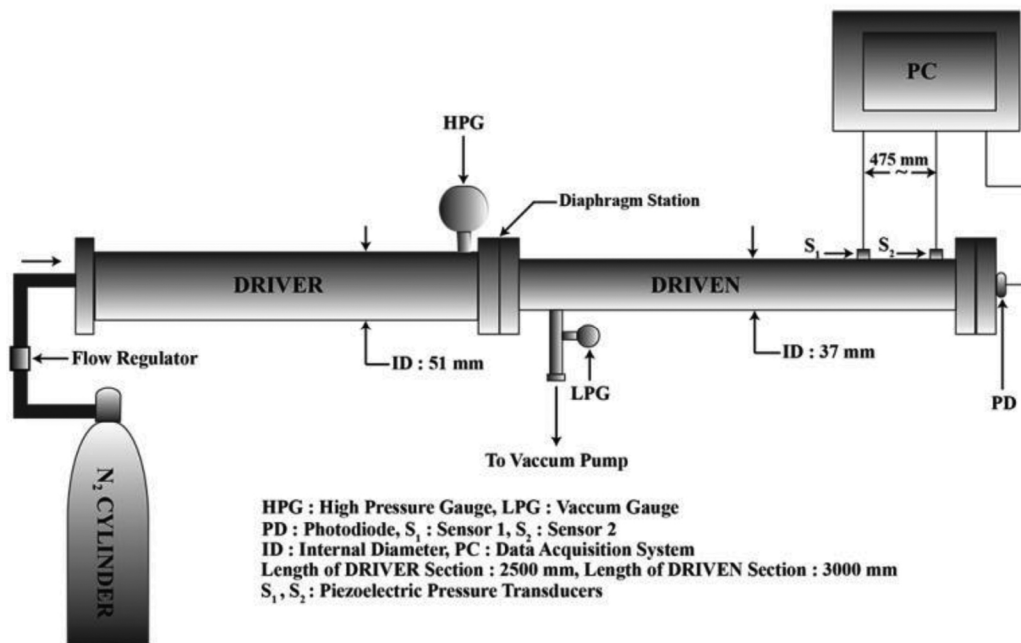
Figure 1. Schematic of the shock tube used for ignition studies.
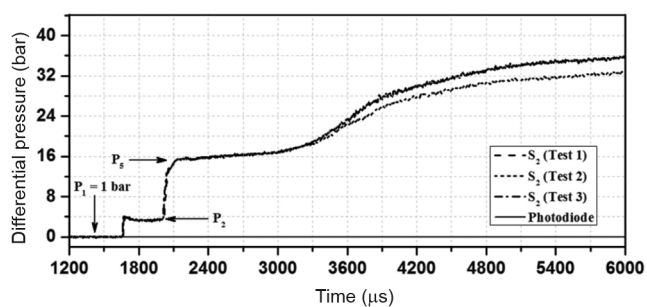
Figure 2. Output of the pressure transducer S_2 during dry runs. P is the test gas pressure. Suffix – 1, Initial; 2, Across incident shock; 5, Reservoir (across reflected shock). Test condition: First condition in Table 1.

the pressure ahead and behind the shock wave respectively[4]

$$\frac{T_b}{T_a} = \frac{P_b}{P_a} \left(\frac{\frac{\gamma+1}{\gamma-1} + \frac{P_b}{P_a}}{1 + \frac{\gamma+1}{\gamma-1} \times \frac{P_b}{P_a}} \right). \quad (2)$$

Table 1 presents the typical dry run conditions.

Figure 3 presents the typical pressure and photodiode traces for fuelled runs for ATF and ATF + Al_2O_3 nanofuel. The output of pressure transducer S_2, which is in the zone of the fuel, is presented in the plots. The photodiode signal plots the line emissions from CH* chemiluminescence of 430 ± 5 nm wavelength ($A^2\Delta \rightarrow X^2\Pi$) that were emitted as soon as the combustion was initiated by the conditions behind the reflected shock wave. The CH* emissions are marked by the near-vertical rise in the output of the photodiode, which is followed by a rise in pressure. The projection of the initial point of rise of the photodiode trace onto the pressure trace (S_2) gives the magnitude of conducive pressure for the initiation of CH* emissions. This pressure is denoted by P_{5i} in Figure 3. It can be observed by a comparison of Figures 2 and 3 that the magnitude of P_{5i} and the trend of pressure prior to this point are identical for dry and fuelled runs. Hence, the variation observed in the trend beyond P_{5i} in Figure 3 could be attributed to the heat release due to a predominant ignition. The ignition delay for the present study is defined as the time between the pressure jump due to the first reflection of the shock wave and the point of

Table 2. Ignition conditions in the shock tube for base- and nano-fuels

Fuel	Volume (ml)	P_{5i} (bar)	T_{5i} (K)	Ignition delay (ms)
ATF	0.257	34.28 ± 4.28%	1007.6 ± 1.58%	2.28 ± 5.24%
ATF + Al_2O_3	0.26	35.08 ± 2.79%	1006.11 ± 1.26%	2.52 ± 10.65%
ATF	0.2	29.403 ± 1.27%	1039.87 ± 1.2%	1.93 ± 4.65%
ATF + Al_2O_3	0.204	28.097 ± 1.32%	1011.81 ± 1.26%	1.967 ± 6.12%

Equivalence ratio = 1. P_{5i}, T_{5i}, Pre-ignition pressure and temperature. ATF, Aviation turbine fuel.
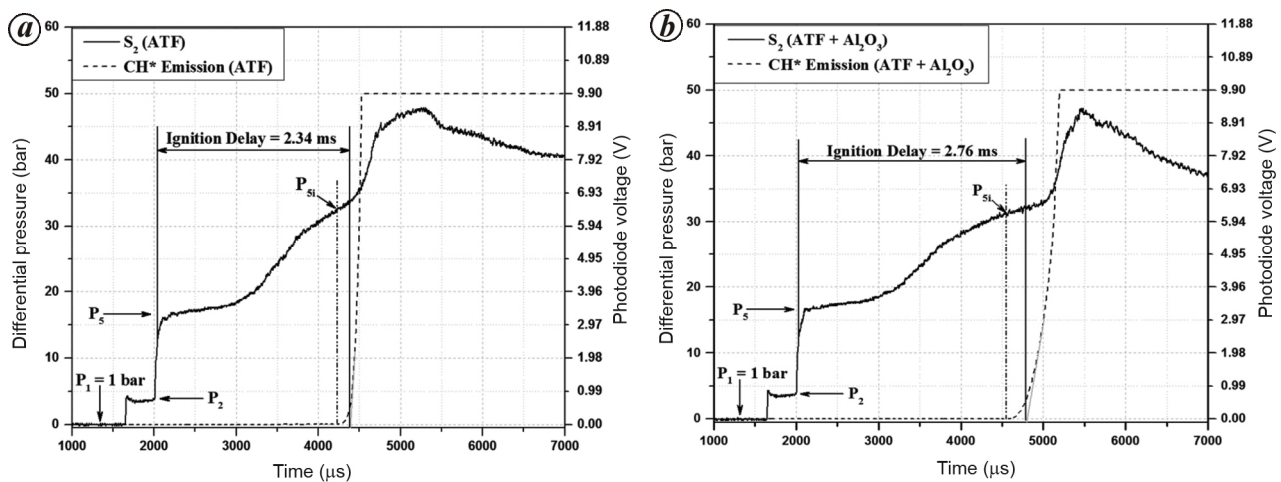
Figure 3. Pressure transducer and photodiode signals during fuelled runs. *a*, Base-fuel, aviation turbine fuel (ATF), first test condition in Table 2. *b*, Nano-fuel, ATF + Al_2O_3, second test condition in Table 2.
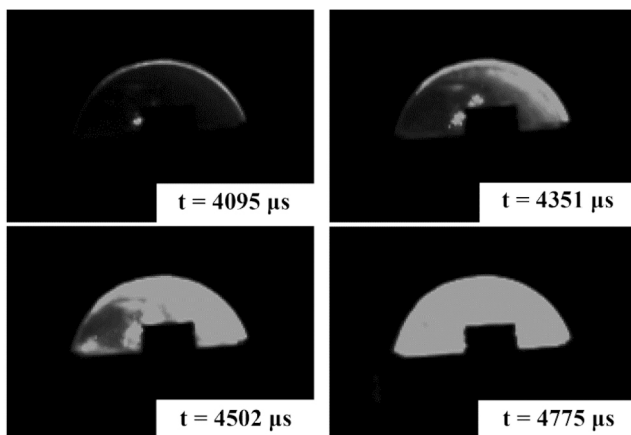
Figure 4. Images of ignition of nano-fuel in the shock tube. Test condition: Second test condition in Table 2.

intersection of the line of extrapolation of the maximum slope of the photodiode trace with the baseline (*x*-axis)[5,6], as shown in Figure 3. The temperature T_{5i}, which corresponds to the pressure P_{5i}, can be calculated using eq. (2), assuming perfect gas conditions. The experimental range of T_{5i} and P_{5i} was 990–1055 K and 27–36 bar respectively. Table 2 presents the test conditions for the fuelled runs. Ignition delay data are also presented in the table.

The acquired data of ignition delay contains an added component of physical delay along with the chemical delay. This physical delay is the time taken by the liquid fuel (droplet) to vapourize before initiation of the chemical process. The visualized images of ignition of the liquid nano-fuel (ATF + Al_2O_3) in the shock tube are presented in Figure 4, for an equivalence ratio of unity. The visualized images exhibit coherence with the output of the photodiode. The data acquired indicate that the nano-fuel can be an alternative for high-speed combustion at temperatures beyond 950 K. This magnitude of temperature is quite common in pulse detonation engines[7–9], where the ATF + Al_2O_3 nano-fuel may find a potential application as a regenerative coolant and a fuel for efficient combustion. The presence of nanoparticles increases the thermal diffusivity of ATF, which in turn increases its rate of heat uptake. Sonawane *et al.*[2] showed that the thermal diffusivity of the nano-fuel increased by 8.4% at 30°C and 24% at 50°C with respect to the base-fuel, i.e. ATF. The increase in thermal diffusivity maintains the ignition delay of the nano-fuel consistent with that of its base-fuel, despite the presence of an inert third body, while enhancing the regenerative cooling capacity of the nano-fuel.

In summary, we measured the ignition delay of a nano-fuel, made of ATF and alumina, to ascertain its suitability for high-speed propulsive applications. The nano-fuel

was produced to enhance the regenerative cooling capacity of the ATF. The study, which was comparative in nature, revealed a meagre increase in the ignition delay of the nano-fuel with respect to ATF (base-fuel), at temperatures (T) > 950 K. The study indicates a negligible compromise on the ignition delay, as against a substantial improvement in the regenerative cooling capacity of the fuel.

1. Nagaboopathy, M., Vijayanand, C., Hegde, G., Reddy, K. P. J. and Arunan, E., Single-pulse chemical shock tube for ignition delay measurements. *Curr. Sci.*, 2008, **95**(1), 78–82.
2. Sonawane, S., Bhandarkar, U., Puranik, B. and Kumar, S. S., Convective heat transfer characterization of aviation turbine fuel–metal oxide nano-fluids. *J. Thermophys. Heat Transfer*, 2012, **26**(4), 619–628.
3. Milton, B. E., Atomization of liquid droplets on surfaces exposed to moving shock waves. *Shock Waves*, 2006, **16**(2), 95–107.
4. Anderson Jr, J. D., In *Modern Compressible Flow: With Historical Perspective* (eds Beamesderfer, L. and Morriss, J. M.), McGraw-Hill, Singapore, 1990, 2nd edn, pp. 209–212.
5. Gauthier, B. M., Davidson, D. F. and Hanson, R. K., Shock tube determination of ignition delay times in full-blend and surrogate fuel mixtures. *Combus. Flame*, 2004, **139**(4), 300–311.
6. Vandersickel, A. *et al.*, The autoignition of practical fuels at HCCI conditions: high-pressure shock tube experiments and phenomenological modeling. *Fuel*, 2012, **93**, 492–501.
7. Litke, P. J., Schauer, F. R., Paxson, D. E., Bradley, R. P. and Hoke, J. L., Assessment of the performance of a pulsejet and comparison with a pulsed-detonation engine. AIAA paper No. 2005-0228.
8. Ma, F., Choi, J. Y. and Yang, V., Thrust chamber dynamics and propulsive performance of single-tube pulse detonation engines. *J. Propulsion Power*, 2005, **21**(3), 512–526.
9. Bussing, T. R. A., Bratkovich, T. E. and Hinkey, J. B., Practical implementation of pulse detonations engines. AIAA paper No. 1997-2748.

Atomic hydrogen storage in a two-dimensional hydrogenated diamond-like carbon film

Nihar Ranjan Ray*

Centre for Indological Studies and Research, The Ramakrishna Mission Institute of Culture, Gol Park, Kolkata 700 029, India

The present communication describes the two-dimensional hydrogenated diamond-like carbon (2D-HDLC) film as a system for storing atomic hydrogen, having hydrogen content in atomic per cent ~37.5 corresponding to gravimetric density of hydrogen ~5.8 wt%.

HYDROGEN is the most promising environmental-friendly 'green' fuel. This is due to the fact that its energy content of 142 MJ per kg exceeds that of petroleum by several factors of magnitude and its combustion produces water vapour only[1]. Electrical energy is produced in a fuel cell due to chemical reaction between oxygen (in air) and hydrogen[2]. Fuel cells are expected to be a practical means for supplying power to road/space vehicles. Therefore, it is necessary for a viable method of on-board hydrogen storage. Currently the methodologies for storing hydrogen in a suitable container are of primary concern. Several means of hydrogen storage were considered using two parameters, viz. gravimetric density (GD), i.e. ratio of weight percentage of hydrogen stored to the total weight of the system (hydrogen + container), and volumetric density (VD), i.e. stored hydrogen mass per unit volume of the system. Till date, hydrogen storage as gas at high pressure or as a liquid at cryogenic temperatures is not found to be suitable for safety and economic reasons. Also, the methods of storing hydrogen in or on solid phase do not fulfil the Department of Energy (DOE), USA targets for GD and VD[3,4]. The well-known diamond-like carbon (DLC) film is referred to as amorphous hydrogenated carbon (a-C: H) film having sp^2 C=C and sp^3 C–H carbons and some films containing up to 50 at% hydrogen[5,6]. The unique properties of a-C: H films make them suitable for various industrial applications[5–7], viz. antireflective, scratch-resistant wear-protective coating, cold cathode material in electron devices, biomedical devices, etc. The amorphous DLC (a-C: H) film was not reported[5–7] for application as hydrogen-storage material[8] in hydrogen-fuel technologies[1]. Since the discoveries of (i) experimental synthesis of graphene[9] (two-dimensional one-atom-thick layer of carbon in hexagonal crystalline structure), and (ii) theoretical prediction of graphane[10]

*e-mail: niharranjanray535@gmail.com